QSCIENCE connect
A Qatar Foundation Academic Journal

OPEN ACCESS

Research article

Land degradation severity assessment with sand encroachment in an ecologically fragile arid environment: a geospatial perspective

Prem Chandra Pandey[1,*], Meenu Rani[2], Prashant Kumar Srivastava[3], Laxmi Kant Sharma[4], Mahendra Singh Nathawat[5]

[1]Department of Geography, University of Leicester, University Road, Leicester, LE1 7RH, United Kingdom
[2]Sustainable development of water resource, Agriculture and forest Project Directorate for Farming Systems Research (PDFSR) Affiliated with ICAR, New Delhi, India
[3]Department of Civil Engineering, Queen's Building, University of Bristol, Bristol, United Kingdom
[4]Centre for Land Resource Management, Central University of Jharkhand, Brambe-835205 Ranchi, India
[5]Department of Geography, School of Life Sciences, Indira Gandhi National Open University, Maidan Garhi, New Delhi-110068, India
*Emails: prem26bit@gmail.com; pcp6@le.ac.uk

ABSTRACT

The objective of this study is to evaluate sand encroached degradation in arid-land, with a predominantly agricultural ecosystem, using geospatial technologies. The study primarily involves the assessment of land degradation severity, severity change dynamics and temporal land-use change patterns, such as growth or shrinkage. Land use/land cover (LULC) change dynamics were analyzed for eight featured classes, derived using a K-means supervised classification method. Overall accuracy and kappa statistics obtained were 91.68% and 0.904 for the year 2001, while 90.85% and 0.896 for year the 2006. The analysis revealed that change dynamic patterns were highest for sand-affected areas and built-up classes, showing positive trend and an overall change of 8.92% and 5.34%, respectively. Degradation severity change dynamics and change patterns clearly showed an increasing trend in highly severe degradation areas (dynamic change 5.55 km^2/change pattern 0.093%), followed by severe degradation (dynamic change 31.22 km^2/change pattern 0.52%). However, the maximum change was observed in moderately severe zones.

Keywords: ecological fragile environment, normalized difference sand dune index, crust index, grain size index, geospatial approach, land degradation severity

http://dx.doi.org/10.5339/connect.2013.43

Submitted: 5 July 2013
Accepted: 5 September 2013

QSCIENCE.com
Member of Qatar Foundation

Cite this article as: Pandey PC, Rani M, Srivastava PK, Sharma LK, Nathawat MS. Land degradation severity assessment with sand encroachment in an ecologically fragile arid environment: a geospatial perspective, *QScience Connect* 2013:43 http://dx.doi.org/10.5339/connect.2013.43

INTRODUCTION

Arid and semi-arid climatic regions are more susceptible to environmental changes, such as degradation and conversion from one land use to another, and even desertification over a long time period.[1] In the diverse climatic zones of India, study areas have arid and semi-arid climatic conditions, where degradation prevailing conditions make these areas interesting to research. Total degraded land in India caused by various factors, such as sand spread, salt affected, waterlogged areas, ravine lands and shifting cultivation is estimated to be 175 million hectares.[2] Degradation is affected by many driving forces, directly or indirectly, these include soil condition, water availability, vegetation covers, biodiversity loss and socio-economic conditions.[3] The severity level of land degradation is also caused by sand drift potential[4] and the migration of sand dunes.[5] However, it has been proved that there is no systematic sand encroachment that would cause desertification.[6] Sand encroached degradation means degradation caused by sand that covers land that was previously devoid of sand, sometimes resulting in desertification. Responses from these driving factors lead to stress conditions which severally impact land-use categories and their utilization, causing degradation either through soil loss (erosion, sealing, movements) or soil conversion (acidification, etc.).[3] Dregne,[7] worked on the degradation classification system based on vegetation covers, climax species and others. Grazing cattle are common in these areas and will destroy vegetation due to pastoral activities of the nomadic societies.[8] Ho and Azadi,[9] consider the role of natural factors such as temperature, wind velocity, rainfall, as well as socio-economic factors. Azadi et al.,[10] demonstrated the intensified loss of agricultural land in developing countries which was in rapid economic growth, and are going through a transition state in their economic structure. Ram and Kolarkar,[11] monitored land-use changes in arid Rajasthan using Landsat and LISS-II images during 1979–1990 and in other study they concluded the sharp depletion and decline in ground water which render fertile irrigable crop-fields in to dry land.[12] There is indication of steep-line shift from sub-humid to arid climate in Jhalawar District near Jhunjhunu, Rajasthan.[13] Ram[14] has also visually interpreted Landsat MSS satellite images for land-use changes in Siwana region, Barmer district of Rajasthan during 1972–1975. Kumar et al.[15] demonstrated desertification in the region due to sand dune movement and confirmed its spread during summer time is more than winter where vegetation covers decreases. Ram and Kolarkar[11] estimated increase of dry land in arid region during 1979–1990, which was later confirmed due to sharp decline in ground water.[12] The changing land use pattern of the region is examined in relation to the trends in rainfall and temperature in and around the region.[16]

Degradation monitoring and assessment along with soil analysis and vegetation complexity were performed in semi-arid zones using Landsat imagery.[17] Raina et al.[18] used Landsat TM imagery to map the type, extent and degree of degradation. Use of multi-sensor and temporal satellite data sets also provides tools for future prediction of regions susceptible to desertification.[19,20] Incorporation of temporal datasets has become an important aspect in assessing the change analysis.[21–24] Yang and Lo[25] used an unsupervised classification technique with a GIS-based image reclassification, and subsequently undertook post-classification using GIS overlay to map spatial urban land-use/land-cover changes.[26–28] Analysis of vegetation indices like NDVI for better interpretation has been demonstrated with temporal dataset in arid and semi-arid environment.[29,30] Visible band data provide most accurate information about spectral change of semi-arid or arid area.[31] For example the normalized difference between the visible red and visible blue band can be used to produce a Crust index (CI) equation to distinguish vegetated or water surfaces from bare soil.[32] Many studies were performed with different methods and techniques for studying the migration of sand dunes,[5] modeling of sand movement through deserts sandy desertification using remote sensing and GIS. Traditional methods used were ground verifications, field visits and surveys. These traditional methods were limited by cost and human resources associated with the lengthy duration of the studies.[33] Earlier remote sensing images, like Landsat, having a spatial resolution of 75m could monitor or detect the variation in sand dune and sand spread areas when it has been longer than 30 meters.

In the present study, the land use categories and its change dynamics with spectral information such as NDVI, NDSDI, GSI and CI have been utilized for the degradation assessment and degradation changes pattern in time period 2001–2006.

The study area

The research area is located in the western part of India at 338m above mean sea level spanning the region between 27°38′N and N and 75°02′E to 76°06′E (figure 1(A)). Topographic maps used in this

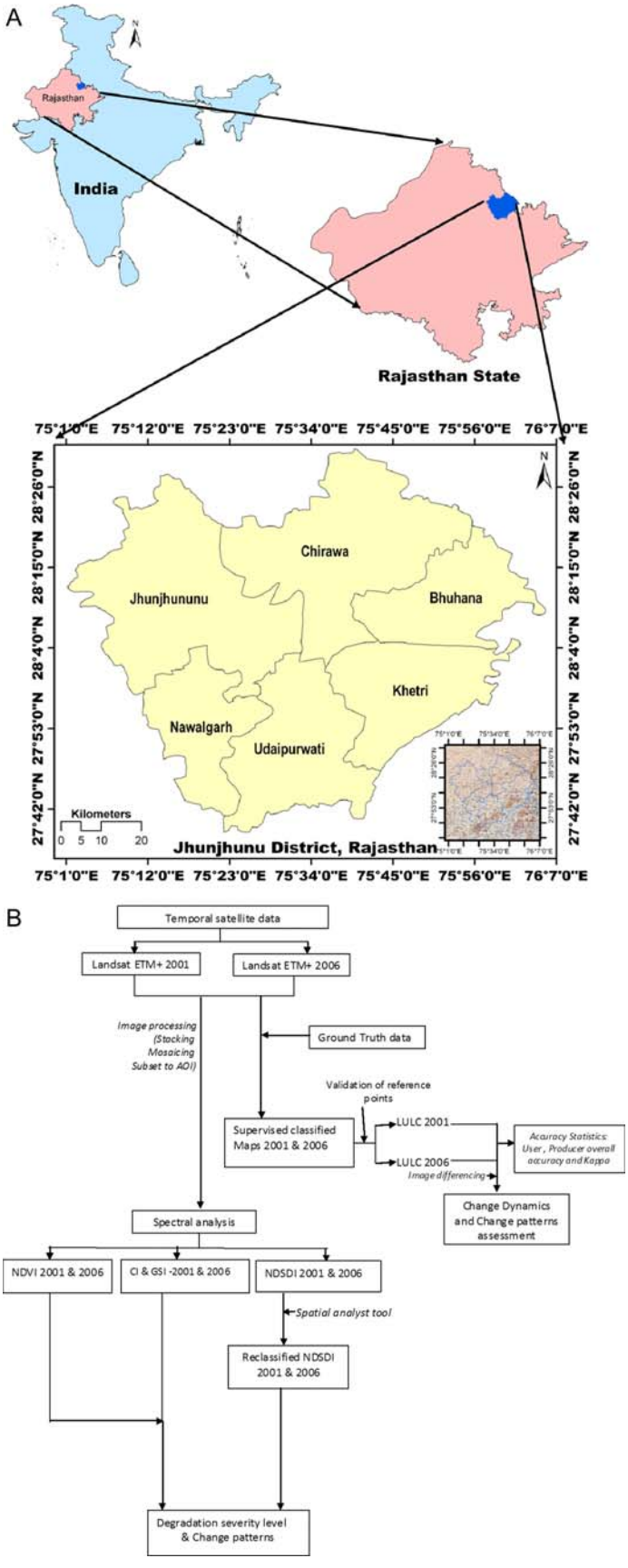

Figure 1. (A) Location map of study site, (B) Methodology adopted in the research.

study were NH 43- 15, and NG 43-3, downloaded from the library of the University of Texas (as shown in inset map of figure 1(B)). The scale of the topographic maps used were 1:250 000. The region is classed as both arid and semi-arid, with minimum temperatures ranging between 2 and 10.5°C during winter, while the maximum temperature ranges between 37 and 45°C during summer. Mean annual rainfall of the region is 444.5 mm. The surface area of Jhunjhunu district is 5,928 sq km, which is 1.73% of the total geographic area of the State Rajasthan. The population in 2001 was 1.91 million, increasing to 2.02 million in 2006, of which 79% was urban population and 26% rural population. Jhunjhunu district has 6 blocks: Nawalgarh, Udaipurwati, Chirawa, Khetri, Jhunjhunu and Buhana.

The landscape of the district comprises of Aeolian plain, rolling hills and pediment areas. The western part of the district (West of river Kantli) consists of sandy plains of Aeolian origin covering almost half of the district area, and the north-eastern part of the district consists of rolling hills. The region experiences different soil types, such as desert soil, which occurs extensively in the central part of the area. These are yellowish-brown in colour, sandy to sandy loam, loose, structure-less and well drained with high permeability. Sand dunes generally found in the northern part of the district covering parts of Buhana and Chirawa blocks. These are non-calcareous soils, sandy to loamy sand, loose, structure-less and well drained lithosols. They are shallow with gravel very near the surface, light textured, fairly drained, reddish brown to grayish brown in colour and belong to the Eutrisol order. Red desertic soil covers parts of the Jhunjhunu and Nawalgarh blocks. These are pale brown to reddish brown in colour, structure-less, loose and well drained, having texture from sandy loam to sandy clay loam. Older Alluvial soil is found in the southern most part of the area, namely in the Khetri, Udaipurwati and Nawalgarh blocks. They are derived from alluvium and are non-calcareous, semi-consolidated to unconsolidated brown soils, loamy sand to sandy loam in texture. North-eastern parts of the district are covered with sandy soil and longitudinal dunes. These regions were characterized by very low rainfall, high air and soil temperature, intense solar radiation and high wind velocity. Wind direction in Jhunjhunu is south-west to north-east. Agricultural activity is spread over both kharif and rabi cultivation. Kharif cultivation is rain-fed and rabi cultivation is generally based on ground water. The region is confronted with primary challenges of degradation because of a fragile ecological environment due to the arid climate, water deficiency, drifting and accumulation of sands. The above reasons make this site interesting and the motivation for the study.

MATERIALS AND METHODS

Remote sensing data acquisition and pre-processing

The study was conducted using Landsat ETM+ satellite data from the year 2001 and 2006, available from the Global Land Cover Facility. The images have a spatial resolution of 30m and a spectral range between 0.45 – 2.35 μm. Full satellite coverage of the study area was performed with four mosaicked Landsat scenes (each scene covering a 185 $km^2 \times 185\ km^2$ area). A vector layer describing the spatial extent of Jhunjhunu was used to subset the imagery to the area of interest (AOI). Correction to the satellite imagery includes image enhancements and atmospheric corrections. The radiance images were converted into reflectance images used for spectral information and analysis.

Dynamic change analysis

Land features change from one feature to another due to natural disturbances or human-induced phenomenon, which results in dynamic change. The pattern of dynamic change is based on the amount of change observed between the time intervals. If the change is increasing then it is positive or if it is towards a decreasing trend, then changes are negative.

Land use/land cover classification

LULC maps were generated from 2001 and 2006 Landsat ETM+ imagery using training samples, and supervised classification was performed with maximum likelihood classification (figure 1(B)). Spectral signatures were recorded for each class as training pixels and subsequently validated for accuracy assessment. The temporal classified images were used for differentiating different feature changes over 6 years. The image differencing techniques were applied on, before and after image, using thematic

properties. The user accuracy, producer accuracy, error of commission, error of omission, overall accuracy and kappa statistic were computed for the reference and classified classes.[34] Errors of commission refer to pixels that belong to another class but were incorrectly labeled as belonging to another class. An error of omission refers to pixels that belong to a particular class but fail to be included within that class.[35] Kappa coefficient (K) is a discrete multivariate measurement technique (Eq. 1) used in accuracy assessments.[36] For instance, $K > 0.80$ represents a strong agreement and good accuracy with the results, if K is between 0.40–0.80 the result is middle ground and $K < 0.40$ is in poor agreement with the results.

$$\text{Kappa statistics (coefficient of agreement)} = \kappa = \frac{N\sum_{i=1}^{r} xii - \sum_{i=1}^{r}(x_{i+} * x_{+i})}{N^2 - \sum_{i=1}^{r}(x_{i+} * x_{+i})} \quad (1)$$

Where, r is the number of rows in the matrix, x_{i+} are the marginal totals of row I, x_{+i} are the marginal totals of column i, x_{ii} is the number of observations in row i and column I, and N is the total number of observations.

Spectral Indices

The satellite images were processed accordingly for calculating spectral indices including NDVI (normalized difference vegetation index) and NDSDI (normalized difference sand dune index) using ERDAS IMAGINE® 9.1 and ESRI's ARC GIS® software.

Normalized Difference Vegetation Index

NDVI vegetation index was applied in the study for the purpose of vegetation analysis- agricultural and forest parts. The index is based on the normalized difference between the RED and the NIR spectral values, which are based on the reflectance in near infrared radiation and the red visible range.[37] Jackson and Huete[38] reported that successful use of indices require knowledge of units of input variables, as well as an understanding how external environment and the architectural aspects of vegetations canopy influence and alter the computed index values. These all depend upon the internal structure of leaves and water content. NDVI is expressed as:

$$\text{NDVI} = \frac{\text{NIR} - \text{RED}}{\text{RED} + \text{NIR}} \quad (2)$$

Where RED is the reflectance of red (band3: 0.63–0.69 μm), and NIR is the near infrared (band4: 0.75–0.90 μm) of the Landsat ETM+ sensors. The differential reflectance in these bands provides a means of monitoring density and vigor of vegetation.[39,40] Values from −1 to 0 (zero) demark areas with no vegetation and values from 0 to +1 represent vegetated areas.

Crust Index

Crust Index (CI) (Eq. 3) is based on the normalized difference between the red and the blue spectral values of the imagery.[32] CI, when applied to the remote sensing imagery, is capable of detecting and differentiating between different lithologic/morphologic units, such as active crusted sand areas, which are expressed in the topography. Karnieli[32] demonstrated that CI is a powerful index to map geological features and is more sensitive to ground features than the wavebands comprising the original image. The CI value ranges between 0 to +2, but typically is between 0 and 1.

$$\text{CI} = 1 - \left(\frac{\text{Red} - \text{Blue}}{\text{Red} + \text{Blue}}\right) \quad (3)$$

Grain Size Index

The GSI was specifically designed for using Landsat TM/ETM + data. The GSI is as follows:

$$\text{GSI} = \left(\frac{\text{Red} - \text{Blue}}{\text{Red} + \text{Green} + \text{Blue}}\right) \quad (4)$$

Where, R, B, and G are the reflectance of the red, blue and green bands of the Landsat TM and ETM+ sensors. GSI value is close to 0 or a smaller value in vegetated area, and for a body of water it is a negative value. Higher positive values of GSI represent the sand affected region.[41] The difference between band R and B in the GSI equation illustrates the difference between vegetated or water surface and bare soil, while the accumulation of the reflectance in the R, G and B bands helps in differentiating the topsoil with different grain size composition.

Normalized Difference Sand Dune Index

To identify and assess the existence of the sand dune accumulations and sand spread, a new index NDSDI[42] is used in this study. The suggested index based on the normalized difference between the RED and the short wave infrared (SWIR) spectral values. This index is aimed at differentiating between sand dune accumulations, bare soils, and other types of soil. NDSDI can be expressed as:

$$\text{NDSDI} = \frac{\text{R} - \text{SWIR}}{\text{R} + \text{SWIR}} \tag{5}$$

Where R is the reflectance of red (band3: 0.63–0.69 μm) and SWIR is the short wavelength infrared (band7: 2.08–2.35 μm) of the Landsat ETM+ sensors. NDSDI mainly distinguishes vegetation and non-vegetation, water and arid surface, sandy or bare soil, while reflectance in the RED and SWIR bands can discriminate the mineral and rock types as it is sensitive to the moisture content of soil and vegetation. Value of the NDSDI ranges between -1 and $+1$, whereas the sand dune accumulations and drifting sands often give values below zero and vegetative cover produces values greater than zero. The NDSDI images were further reclassified into six levels of sand induced degradation severity using spatial analyst function within ArcGIS software. The values ranging from -1 to <0 were classified as level-I to level-IV, where values of <0 were classified to Level-I to level-III. The range value >0 falls into vegetation cover and they are classified into level-V and VI (as they are normal with no degradation). The degradation severity levels were classified as follows: Level-I (highly severe), Level-II (severe), Level-III (moderately severe), Level-IV (highly susceptible to degradation), Level-V (less susceptible to degradation) and Level-VI (No degradation).

RESULTS AND DISCUSSION

Pattern and dynamic changes in land use/land cover between 2001 and 2006

The supervised LULC maps of 2001 and 2006 in the study site are depicted in figure 2(A, B). Accuracy assessment for user, producer, overall and kappa accuracy achieved for individual land use class is based on the error matrix (tables 1, 2). Overall user accuracy and overall producer accuracies were 90.09% and 91.76%, respectively, for land use achieved in 2001. Imagery and accuracies of 84.50%

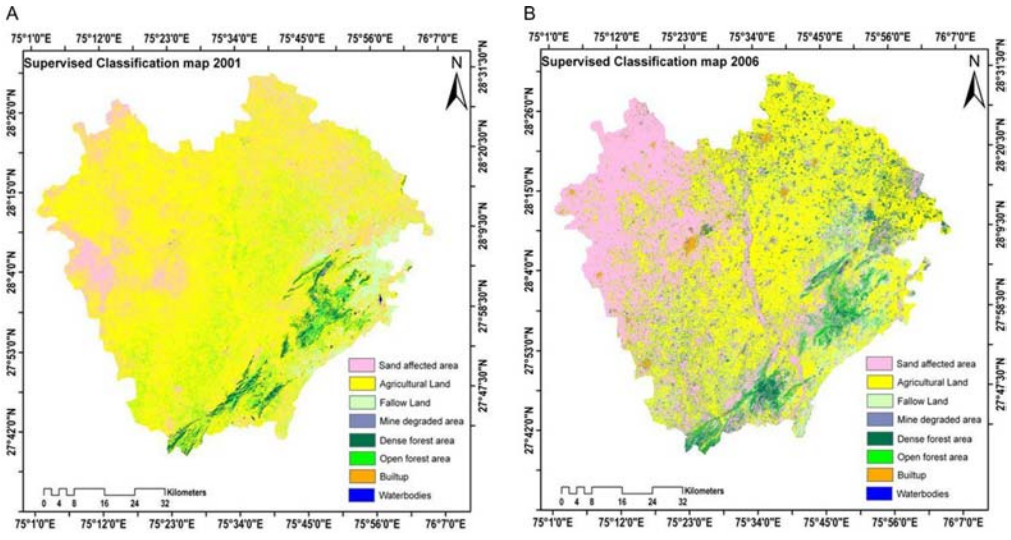

Figure 2. (A) Supervised classification map 2001, (B) Supervised classification map 2006 and Tables 1, 2 and 3.

Table 1. Error matrix for accuracy assessment of supervised classified image 2001.

Classified data	Built-up	Mine degraded area	Sand affected area	Fallow Land	Water bodies	Dense forest	Open forest	Agricultural area	(Classified) Row total	User Accuracy of each class
Built-up	437	10	8	6	2	0	0	15	478	**91.42**
Mine degraded area	0	544	109	0	23	0	0	0	676	**80.47**
Sand affected area	2	71	2354	116	0	0	0	11	2554	**92.174**
Fallow Land	0	0	0	2559	0	0	0	69	2628	**97.37**
Water bodies	0	0	89	0	1281	0	0	0	1370	**93.50**
Dense forest	0	0	0	0	4	2957	182	22	3165	**93.43**
Open forest	0	0	0	0	0	60	1240	246	1546	**80.21**
Agricultural area	5	0	15	91	0	27	98	2754	2990	**92.11**
(Reference) Column total	444	625	2575	2772	1310	3044	1520	3117	**15407**	
Producer Accuracy of each class	**98.42**	**87.04**	**91.42**	**92.32**	**97.79**	**97.14**	**81.58**	**88.35**		

Mean user accuracy = 90.08%, Error of commission = 9.92%, Mean producer accuracy = 91.76%, Error of omission = 8.24%, Overall accuracy = 91.69%, Kappa statistics = 0.90.

Table 2. Error matrix for accuracy assessment of supervised classified image 2006.

Classified data	Built-up	Mine degraded area	Sand affected area	Fallow Land	Water bodies	Dense forest	Open forest	Agricultural area	(Classified) Row total	User Accuracy of each class
Built-up	2904	51	213	184	0	0	2	95	3449	**84.20**
Mine degraded area	14	1289	13	2	0	0	0	4	1322	**97.50**
Sand affected area	1	197	1323	0	0	0	0	0	1521	**86.98**
Fallow Land	10	0	0	4679	2	0	0	93	4784	**97.81**
Water bodies	9	5	0	143	448	1	4	28	638	**70.22**
Dense forest	1	0	0	9	2	2196	0	0	2208	**99.46**
Open forest	53	1	0	3	4	0	170	87	318	**53.46**
Agricultural area	24	0	1	168	12	0	13	1381	1599	**86.37**
(Reference) Column total	3016	1543	1550	5188	468	2197	189	1688	**15839**	
Producer Accuracy of each class	**96.29**	**83.54**	**85.35**	**90.19**	**95.73**	**99.95**	**89.95**	**81.81**		

Mean user accuracy = 84.50%, Error of commission = 15.50%, Mean producer accuracy = 90.35%, Error of omission = 9.65%, Overall accuracy = 90.85%, Kappa statistics = 0.90.

Table 3. LULC map area statistics in 2001 and 2006 and change statistics of each class with time period.

Sl	Land use land cover	2001		2006		Change Dynamics (km^2)(3 – 1)	Change pattern of each classes of LULC (in percentage) (4 – 2)	Status
		1. Area (km^2)	2. Percentage of area in LULC	3. Area (km^2)	4. Percentage of area in LULC			
1	Built-up	112.151	1.893	428.917	7.239	316.766	5.346	+ Increased
2	Mine degraded area	20.256	0.341	24.674	0.416	4.418	0.074	+ Increased
3	Sand affected area	1819.033	30.703	2347.820	39.627	528.786	8.924	+ Increased
4	Agricultural area	2264.395	38.220	1751.961	29.570	− 512.433	− 8.650	− Decreased
5	Fallow Land	973.941	16.439	829.113	13.994	− 144.827	− 2.444	− Decreased
6	Water bodies	1.915	0.032	2.651	0.044	0.736	0.012	+ Increased
7	Open forest	69.261	1.169	198.291	3.346	129.030	2.177	+ Increased
8	Dense forest	663.588	11.200	341.261	5.759	− 322.326	− 5.440	− Decreased
		5924.545	100	5924.693	100	–	–	–

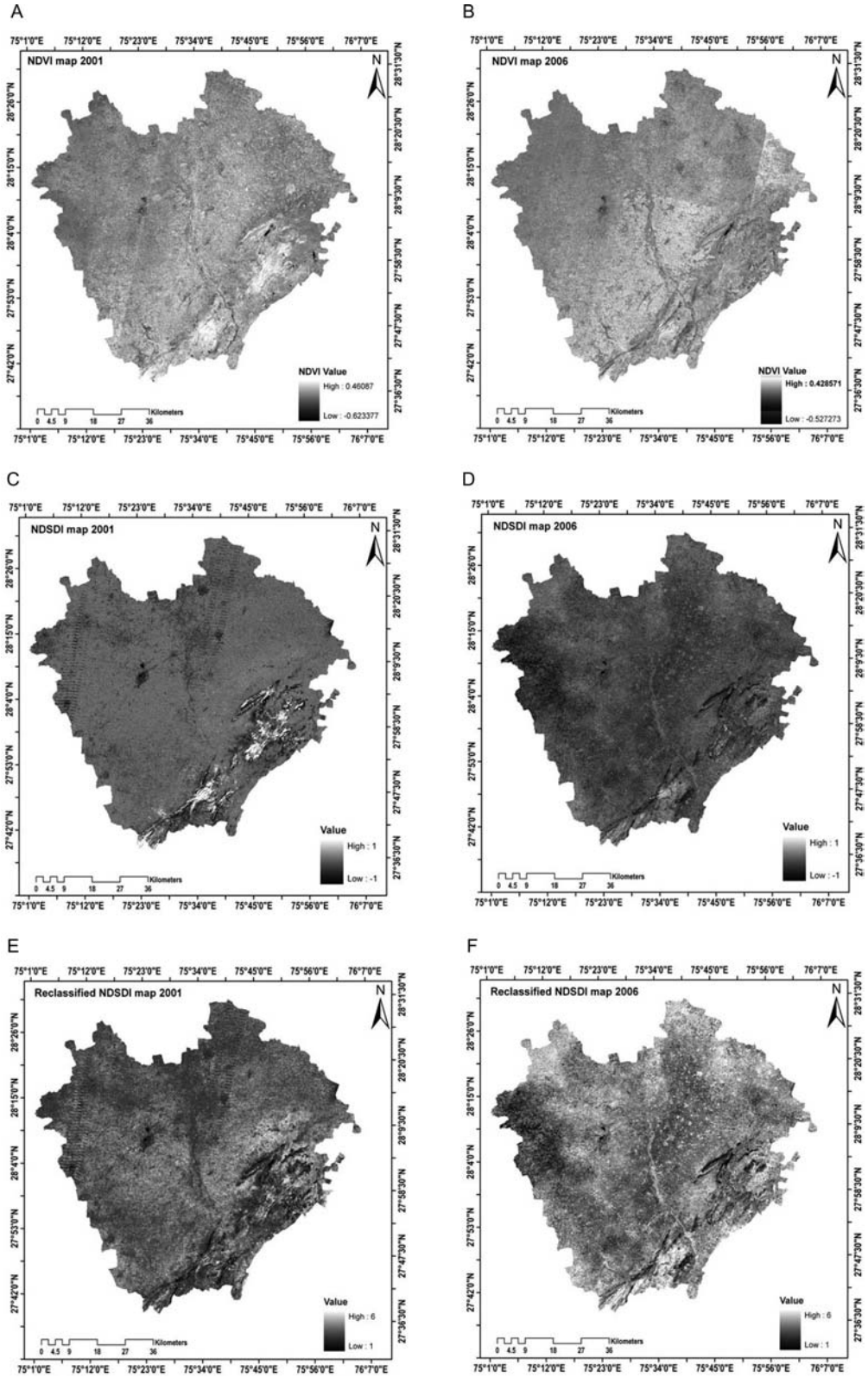

Figure 3. Spectral maps of the area: (A) NDVI map 2001, (B) NDVI map 2006, (C) NDSDI map 2001, (D) NDSDI map 2006, (E) Reclassified NDSDI map 2001, and (F) Reclassified NDSDI map 2001 and Table 4.

Table 4. Changes dynamics and severity pattern of sand dune degradation in 2001 and 2006.

	1	2	3	4	5	6	7	8
Severity level	Rank level	Area in 2006 (km^2)	Percentage of severity in 2006 [(2/5919.058)*100]	Area In 2001 (km^2)	Percentage of severity in 2001 [(4/5919.058)*100]	Severity change dynamics (2−4)	Amount of Severity area change (3−5)	Pattern of Changes in 6 year
Highly severe	level-I	23.797	0.402	18.239	0.308	5.558	0.093	+ Increased
Severe	level-II	100.593	1.699	69.366	1.171	31.226	0.527	+ Increased
Moderately severe	level-III	3280.240	55.41	451.788	7.632	2828.452	47.785	+ Increased
Highly susceptible to degradation	level-IV	2054.824	34.715	1655.552	27.969	399.271	6.745	+ Increased
Less susceptible to degradation	level-V	389.415	6.579	2153.993	36.390	−1764.577	−29.811	− Decreased
No degradation	level-VI	70.186	1.1857	1570.118	26.526	−1499.932	−25.340	− Decreased
Total area		5919.058		5919.058		−		

Table 5. Sand Spread Severity extent in the study area in 2006 and 2001.

	Navalgarh block		Udaipurwati block		Chirawa block		Khetri block		Jhunjhunu block		Buhana block		Total severity area	
	Area in (km^2)		Area in (km^2)		Area in (km^2)		Area in (km^2)		Area in (km^2)		Area in (km^2)		Area in (km^2)	
Severity level	**2006**	**2001**	**2006**	**2001**	**2006**	**2001**	**2006**	**2001**	**2006**	**2001**	**2006**	**2001**	**2006**	**2001**
Highly severe	2.092	0.905	4.473	4.350	1.025	1.632	8.862	8.111	5.940	0.404	1.403	2.836	**23.797**	**18.239**
Severe	6.826	5.946	4.709	2.988	6.077	5.944	19.424	3.316	54.318	45.298	9.237	5.872	**100.593**	**69.366**
Moderately severe	162.465	25.799	89.120	57.884	1236.614	80.206	722.957	75.931	762.002	160.835	307.079	51.130	**3280.240**	**451.788**
Highly susceptible to degradation	56.234	67.724	345.049	18.670	535.234	504.348	112.818	269.074	622.860	452.229	382.627	343.504	**2054.824**	**1655.552**
Less susceptible to degradation	16.0225	78.275	51.492	223.213	83.261	766.143	88.579	343.010	58.943	510.114	91.116	233.235	**389.415**	**2153.993**
No degradation	21.525	86.513	1.439	189.177	0.984	504.922	18.033	271.233	16.243	351.426	11.959	166.845	**70.186**	**1570.118**
Total Area	**265.166**	**265.166**	**496.284**	**496.284**	**1863.197**	**1863.197**	**970.676**	**970.676**	**1520.308**	**1520.308**	**803.424**	**803.424**	**5919.058**	**5919.058**

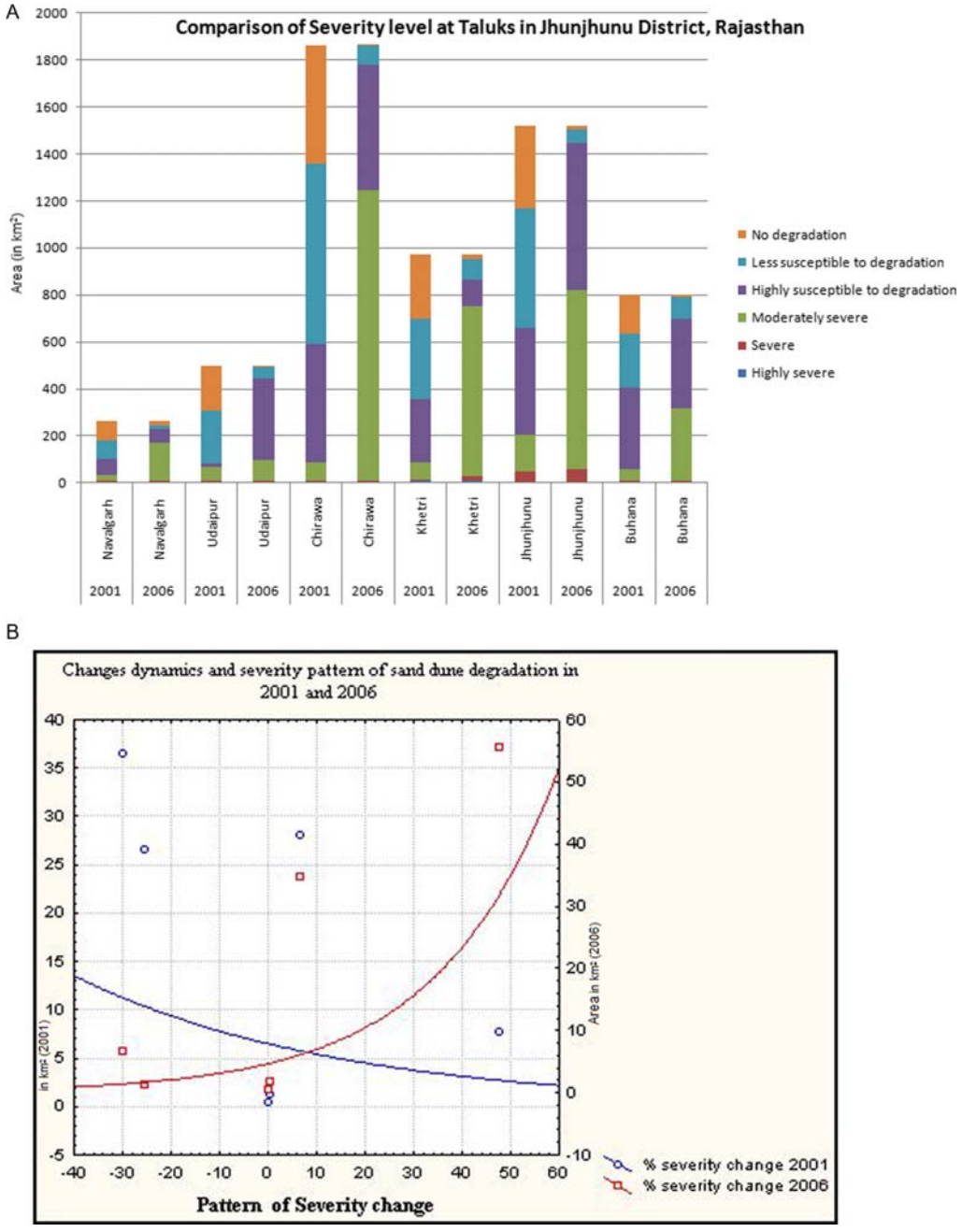

Figure 4. (A) Graph comparison of severity level in blocks and (B) Graph showing change dynamics with severity pattern in blocks in 2001 and 2006. Table 5. CI and severity level of the sand spread in region.

and 90.36%, respectively, were achieved in 2006. Finally, 91.69% for overall accuracy and 0.90 for kappa statistics were achieved for land use cover in 2001, compared to 90.85% and 0.90 in 2006.

Table 3 is relevant in providing the dynamic change and patterns of changes in percentage. The negative change patterns were shown by agricultural area, fallow land and dense forest of −8.650, −2.444 and −5.440 respectively, whereas the positive trend in change patterns were shown by built-up, mine degraded area, sand affected area, water bodies and open forest of 5.346, 0.074, 8.924, 0.012 and 2.177 %, respectively, in the time period of 6 years. The positive trend is shown in sand affected areas with 528.786 km^2 and has gained approximately 8.924 % of total area in the time duration. This change pattern is followed by built-up and open forest with an increase in areal extent of 316.766 km^2 with a gain of 5.346 % and 129.030 km^2 with a gain of 2.177 % of total study area, respectively.

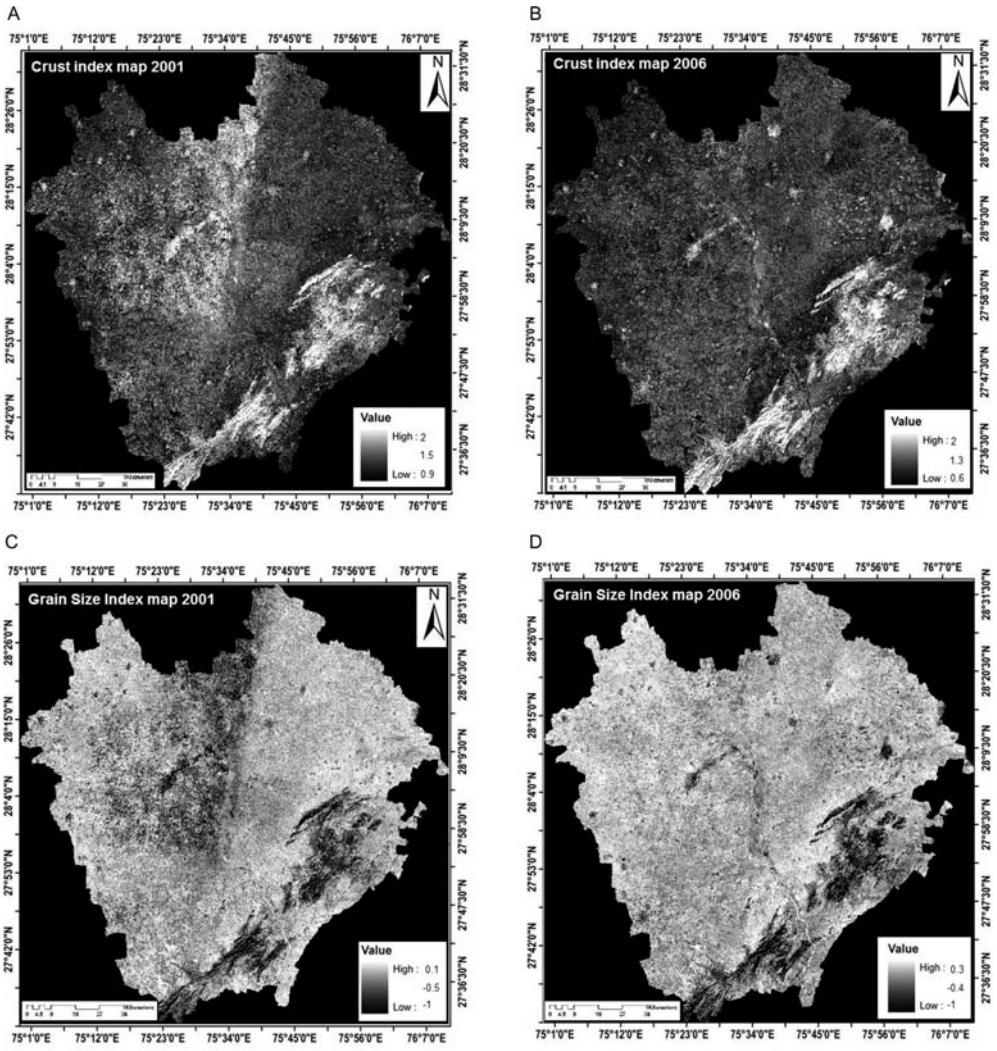

Figure 5. (A) Crust Index map 2001, (B) Crust Index map 2006, (C) Grain Size Index map 2001 and (D) Grain Size Index map 2006.

Vegetation index (NDVI) of the study area

The NDVI maps of the study site were illustrated in figure 3(A, B) for years 2001 and 2006, respectively. NDVI values range from −0.527 to 0.428 for 2001 and −0.623 to 0.460 for 2006. The vegetation, cropland and other plantation areas declined in 2006 and there is an increase in the non-vegetation regions in 2006.

NDSDI and severity level of the sand spread in region

Based on the spectral index result, severity level classifications were done on the 2001 and 2006 indexed maps, shown in figures 3(C), (D), respectively. The NDSDI image is further classified into 6 classes for each respective year as shown in figure 3(E, F). Table 4 illustrates the severity levels that were classified into six levels for 2001 and 2006, whereas table 5 represents the severity level for each block for the two corresponding years. Level I gained in area of 5.558 km^2, with a 0.093 % growth in severity. Level II showed an increase in areal extent of approximately 31.226 km^2 with a positive growth pattern (0.527%). The degradation severity change dynamics and severity change patterns clearly show an increasing trend towards highly severe (5.55 km^2 and increased to 0.093%) and severe level (31.22 km^2 and increased to 0.52%), whereas the maximum increase was seen in the moderately severe zone (2828.45 km^2), which increased to 47.78%. The no degradation and less susceptible zones

have shown a decrease in areal extent to 55.15%. The maximum change is seen in the level III, moderately severe zone, which has gained an area of 2828.452 km^2 with 47.785% degradation severity pattern, which is approximately half of the total values. Likewise, a similar result is shown by level IV. The negative pattern, which clearly depicts the scene of conversion from less susceptible areas to other levels, initially in 2001, show these levels have 36.39% and 26.52% of total area contribution.
The results clearly illustrate that areas from each level have been either converted into other levels naturally and by anthropogenic activities. Table 3 clearly depicts the significant shrinkage in the spatial extent of level V and level VI from 2001 to 2006. Thus, in 2001, total lands which are classified and fall into the categories of less susceptible and no degradation level severity of degradation (sum of level V and level VI) is 3724.11 km^2 (62.91%), whereas in 2006, this area is reduced to only 459.60 km^2 (7.764%). Figure 4(B) illustrates the percentage of degradation severity changes in 2001 and 2006 on double Y-axis, and pattern of severity change in the X-axis.

Comparison of the severity for 2001 and 2006 is shown for the 6 blocks (Nawalgarh, Udaipurwati, Chirawa, Khetri, Jhunjhunu and Buhana) in table 5 and figure 4(A) shows graphical statistics. These areas are moderately severe in each block as they share the maximum percentage in 2006 as compared to 2001. The pattern shown in figure 4(B) and data in table 4 indicate that the severity change in 2006 is continuously increasing towards high degradation. The region in 2001, that was under no degradation or was less susceptible to degradation, is now highly susceptible and moderately degraded. The major concern is the area classed as less or not susceptible in 2001, which was approximately 62%, this remains only 7.7% in 2006, showing the rest of area is moderately and highly susceptible to degradation. The trend is changing from less to more in terms of degradation, as shown through the red line in figure 4(B). Chirawa block has an increased area with no degradation in 2001 but less areas are under no degradation in 2006 as compared to other blocks. Figure 4(A) clearly shows that no degradation area is affected in every block and decreased in its extent in 2006 compared to 2001. But the most affected blocks were Chirawa, Udaipur, Jhunjhunu and Buhana.

Figures 5(A, B) illustrate the CI maps of Landsat image 2001 and 2006 based on the normalized difference of red and blue bands. The result ranges from 0.9 to 2 in 2001 and 0.6 to 2 in 2006. The dense forest and agricultural regions show high values of the CI, up to 2, whereas desert prone and degraded areas affected with sand encroachments show lower CI values, i.e. 0.9 in 2001 and 0.6 in 2006. The CI value difference for 2001 and 2006 is increased up to 0.3 from 2001 to 2006 (0.9 – 0.6), which clearly demonstrates the increase in degradation severity of the region.

GSI and severity level of the sand spread in region

Figures 5(C, D) illustrate the GSI maps of Landsat images 2001 and 2006, based on the normalized difference of red and blue bands. The result ranges between −1 to 0.1 for 2001 and −1 to 0.3 for 2006. The value is negative for dense forest, agricultural region and water bodies. Highly positive values were shown by sandy and degraded areas affected with sand encroachments. The GSI value difference for 2001 and 2006 is increased by up to 0.2, which clearly demonstrates the increase in the degradation severity of the region. Vegetation, dense forest and cropland show smaller GSI values or even negative values for the study area. In contrast to this, sandy, desert area and sand affected regions show higher GSI values, close to 0.1 in 2001 and 0.3 in 2006. Thus, it clearly indicates the accumulation of sand and a clear indication of increasing trend where the sandy content of soil increases with higher GSI values.

CONCLUSION

This study clearly depicts the severity of land degradation due to sand spread in blocks, in the Jhunjhunu district in Rajasthan, representing a threat to the agricultural area and a potential decline in productivities. Increasing land use patterns were affected by the sand encroachment region of India, where degraded land is rapidly expanding. One land feature changes to another either due to natural phenomenon or human-induced phenomenon and results in dynamic change. The pattern is based on the amount of changes from an earlier state to a later state. Either feature extends its occupancy in positive trends or if the feature extent declines compared to earlier status, this represents negative trends. The potential vegetation cover decreases with decreasing species, in frequency and numbers, barren and fallow-land were not untouched by degradation effect. So, vegetation cover is highly susceptible to land degradation, and the same conditions exist for barren and fallow-land. Here, LULC dynamics change patterns and trends were in parallel discussion with land degradation severity changes and patterns. It will be not validated without basic skeleton LULC and its changes patterns in

the region. LULC does have an impact due to land degradation, and it has an impact on vegetation covers, agricultural and fallow-land, which were engulfed by degradation in areas that were considered either highly susceptible or susceptible on occasion to degradation.

The above study shows that land use changes and degradation are interrelated. One factor affects others causing either a decrease or increase. Similarly, land use is converted into other classes during 2001–2006 and their status was changing in either positive or negative trends.

The degradation severity change dynamics and change patterns, as shown in Table 4, clearly indicate an increasing trend for highly severe (dynamic change 5.55 km^2 and change pattern to 0.093%), severe (dynamic change 31.22 km^2 and change pattern 0.52%), whereas the maximum increase was seen in moderately severe zones (2828.45 km^2), which is 47.78%. No-degradation zones and less susceptible zones have shown a decrease in areal extent contributing 55.15% loss to other zone. Similarly table 5 illustrated increase in level 1 (highly severe zone) and decline in the less degradation and no-degradation zones from 2001 to 2006 in blocks of the district. Spectral index CI and GSI were also incorporated to see the degradation severity as well as the sand affected regions as shown in figure 5(A, B, C, D). The vegetation, dense forest, cropland (GSI value $= -0.4$) and water (GSI value $= -0.1$), show smaller or even negative GSI values (GSI value range from -1 to 1). In contrast to this, sandy, desert area and sand affected region shows higher GSI values, close to 0.1 in 2001 and 0.3 in 2006. Thus, it clearly indicates the accumulation of sand and is a clear sign of increasing trend, where sandy content of soil increases with higher GSI values. Similarly CI values of the vegetation, dense forest, cropland in 2001 and 2006 comes to be 2 (higher CI values) and lower CI values of 0.3 and 0.6 is illustrated for the sandy regions in year 2001 and 2006, respectively. Spectral index NDVI was also applied to look for the vegetation aspects and its spread in the region for both years. NDSDI results were interpreted and for achieving the best results, these are again reclassified for exact status of sandy area or degraded area. Based on the above results and discussions, it can be concluded that tendency for degradation has been more in an east direction as well as northeast direction. It can be observed through NDVI maps also, which shows less vegetation in these directions and also through CI and GSI index maps indicating increase in its values towards east and northeast directions. Pattern of change is generally seen in these degraded affected directions as well. It clearly depicts the status of the areas that were classified as lower levels of sand degradation were converted to other higher degraded level. Thus, the use of geospatial techniques provides temporal analysis and region monitoring with synoptic view, for evaluation of sand spread.

REFERENCES

[1] Koch M. Geological controls of land degradation as detected by remote sensing: A case study in Los Monegros, north-east Spain. *Int J Remote Sensing*. 2000;21(3):457–473.
[2] Das DC. Problem of soil erosion and land degradation in India. Proceedings of the National Seminar on Soil Conservation and Watershed Management. Indian Association of Soil and Water Conservationists, New Delhi, India. 1985.
[3] Gobin A, Govers G, Jones R, Kirkby M, Kosmas C. Assessment and reporting on soil erosion. *European Environment Agency, Technical Report*. 2003;94:103.
[4] Al-Awadhi JM, Al-Helal A, Al-Enezi A. Sand drift potential in the desert of Kuwait. *J Arid Environ*. 2005;63(2):425–438.
[5] Yao ZY, Wang T, Han ZW, Zhang WM, Zhao AG. Migration of sand dunes on the northern Alxa Plateau, Inner Mongolia, China. *Journal of Arid Environments*. 2007;70(1):80–93.
[6] Helldén U. Desertification monitoring: is the desert encroaching? *Desertif Control Bull*. 1988;17:8–12.
[7] Dregne HE. Desertification of Arid Lands. Springer-Verlag; 1986; 4–34.
[8] Tsoar H, Karnieli A. What determines the spectral reflectance of the Negev-Sinai sand dunes. *Int J Remote Sensing*. 1996;17(3):513–525.
[9] Ho P, Azadi H. Rangeland degradation in North China: perceptions of pastoralists. *Environ Res*. 2010;110(3):302–307.
[10] Azadi H, Ho P, Hasfiati L. Agricultural land conversion drivers: a comparison between less developed, developing and developed countries. *Land Degrad Dev*. 2011;22(6):596–604.
[11] Ram B, Kolarkar AS. Remote sensing application in monitoring land-use changes in arid Rajasthan. *Int J Remote Sensing*. 1993;14(17):3191–3200.
[12] Ram B, Chauhan JS. Application of remote sensing and GIS to assess land use changes in Jhunjhunun district of arid Rajasthan. *J Indian Soc Remote Sensing*. 2009;37(4):671–680.
[13] Subramaniam AR, Prasada Rao GSLHV. Climatic study of water balance, aridity and droughts in Rajasthan State. *Ann Arid Zone*. 1980;19(4):371–377.
[14] Ram B. Recent changes in land-use in an arid-environment. A case study of Siwana region. Rajasthan, Jodhpur University, Jodhpur, India. Doctoral thesis, 1988.
[15] Kumar M, Goossens E, Goossens R. Assessment of sand dune change detection in Rajasthan (Thar) Desert, India. *Int J Remote Sensing*. 1993;14(9):1689–1703.
[16] Pant GB, Hingane LS. Climatic changes in and around the Rajasthan desert during the 20th century. *J Climatol*. 1988;8(4):391–401.

[17] Fredriksen P. Satellite based assessment and monitoring of land degradation in semi-arid tropical Africa – aspects of the soil/vegetation complex. *EARseL Advan Remote Sensing*. 1993;2(3-XI):102–110.
[18] Raina P, Joshi DC, Kolarkar AS. Land degradation mapping by remote sensing in the arid region of India. *Soil Use Manage*. 1991;7(1):47–51.
[19] Gao J, Liu Y. Mapping of land degradation from space: a comparative study of Landsat ETM+ and ASTER data. *International Journal of Remote Sensing*. 2008;29(14):4029–4043.
[20] Ramsey MS. *Global Desert Monitoring With ASTER; Research Projects*. : Image Visualization and Ifrared Spectroscopy (IVIS) Laboratory, University of Pittsburg; 2003.
[21] Sharma L, Pandey PC, Nathawat MS. Assessment of land consumption rate with urban dynamics change using geospatial techniques. *J Land Use Sci*. 2012;7(2):135–148.
[22] Srivastava PK, Gupta M, Mukherjee S. Mapping spatial distribution of pollutants in groundwater of a tropical area of India using remote sensing and GIS. *Appl Geomat*. 2012;4(1):21–32.
[23] Srivastava PK, Han D, Gupta M, Mukherjee S. Integrated framework for monitoring groundwater pollution using a geographical information system and multivariate analysis. *Hydrol Sci J*. 2012;57(7):1453–1472.
[24] Srivastava PK, Han D, Rico-Ramirez MA, Bray M, Islam T. Selection of classification techniques for land use/land cover change investigation. *Advan Space Res*. 2012;50(9):1250–1265.
[25] Yang X, Lo CP. Using a time series of satellite imagery to detect land use and land cover changes in the Atlanta, Georgia metropolitan area. *Int J Remote Sensing*. 2002;23(9):1775–1798.
[26] Srivastava PK, Mukherjee S, Gupta M. Impact of urbanization on land use/land cover change using remote sensing and GIS: a case study. *Int J Ecol Econ Stat*. 2010;18(S10):106–117.
[27] Gupta M, Srivastava PK. Integrating GIS and remote sensing for identification of groundwater potential zones in the hilly terrain of Pavagarh, Gujarat, India. *Water Int*. 2010;35(2):233–245.
[28] Srivastava PK, Mukherjee S, Gupta M, Singh SK. Characterizing monsoonal variation on water quality index of river Mahi in India using geographical information system. *Water Qual Expo Health*. 2011;2(3-4):193–203.
[29] Elhadi EM, Zomrawi N, Guangdao H. Landscape Change and Sandy Desertification Monitoring and Assessment. *American Journal of Environmental Sciences*. 2009;5(5):633–638.
[30] Chavez PS, MacKinnon DJ. Automatic change detection of vegetation changes in the Southwestern United States using remotely sensed images. *Photogramm Eng Remote Sensing*. 1994;60(5):571–583.
[31] Pilon PG, Howarth PJ, Bullock RA, Adeniyi PO. An enhanced classification approach to change detection in semi-arid environment. *Photogramm Eng Remote Sensing*. 1988;45(12):1709–1716.
[32] Karnieli A. Development and implementation of spectral crust index over dune sands. *Int J Remote Sensing*. 1997;18(6):1207–1220.
[33] Dong Z, Wang X, Chen G. Monitoring sand dune advance in the Taklimakan Desert. *Geomorphology*. 2000;35(3-4):219–231.
[34] Story M, Congalton R. Accuracy assessment: a user's perspective. *Photogramm Eng Remote Sensing*. 1986;52(3):397–399.
[35] Congalton RG. A comparison of sampling schemes used in generating error matrices for assessing the accuracy of maps generated from remotely sensed data. *Photogramm Eng Remote Sensing*. 1988;54(5):593–600.
[36] Bishop Y, Fienberg S, Holland P. *Discrete Multivariate Analysis-Theory and Practice*. Cambridge, MA: MIT Press; 1975: p. 575.
[37] Frantzova A. Remote Sensing, GIS and Disaster Management. Third International Conference on Cartography and GIS. Nessebar, Bulgaria, 2010.
[38] Jackson RD, Huete AR. Interpreting vegetation indices. *Preventive Veterinary Medicine*. 1991;11(3-4):185–200.
[39] Townshend JRG, Justice CO. Analysis of the dynamics of African vegetation using the normalized difference vegetation index. *Int J Remote Sensing*. 1986;7(11):1435–1445.
[40] Thakur JK, Srivastava PK, Singh SK, Vekerdy Z. Ecological monitoring of wetlands in semi-arid region of Konya closed Basin, Turkey. *Reg Environ Change*. 2012;12(1):133–144.
[41] Xiao J, Shen Y, Tateishi R, Bayaer W. Development of topsoil grain size index for monitoring desertification in arid land using remote sensing. *Int J Remote Sensing*. 2006;27(12):2411–2422.
[42] Fadhil AH. Land degradation detection using Geo-information technology for some sites in Iraq. *J Al-Nahrain Univ*. 2009;12(3):94–108.